mapping. Additional polymorphic DNA markers based on repeat sequences were generated for high-resolution mapping (see http://mouse.ski.mskcc.org/).

Molecular identification of *fxo* and *wim*

In a mapping cross of 796 opportunities for recombination, *fxo* was mapped between D14Mit84 and D7Mit111. Products from polymerase chain reaction with reverse transcription (RT–PCR) that were amplified from E10.5 *fxo* embryos lacked the 87-base-pair exon 16 of the *polaris* transcript. Analysis of the genomic sequence surrounding exon 16 identified a T to C mutation in the second nucleotide of intron 16 (downstream of exon 16), which was associated with the skipping of exon 16.

In a mapping cross of 2,600 opportunities for recombination, *wim* was mapped to a 484-kb interval between D5Ski122 and D5Ski114 (see http://mouse.ski.mskcc.org/). The *wim* interval contained 7 known and 14 predicted genes, according to the current genome assembly. We ruled out four genes (*Slc30a3*, *Ucn*, *Mpv17* and *Gckr*) as candidates because mice lacking these genes survive to adulthood[25–28]. Three genes were not expressed in mid-gestation embryos on the basis of RT–PCR analysis of E10.5 RNA. Four predicted genes were not sequenced because their predicted function seemed completely unrelated to Hh signalling or neural tube patterning. The complete coding region of the remaining ten candidate genes was sequenced from RT–PCR products amplified from E10.5 *wim* (six independent embryos sequenced) and parental (C57BL/6) embryos. The only sequence change identified was a T to C substitution in a predicted gene corresponding to five Ensembl predicted transcripts (ENSMUST00000041444, ENSMUST00000041565, ENSMUST00000041704, ENSMUST00000031036 and ENSMUST00000041963) homologous to the full-length rat *SLB* RNA[29]. The change was confirmed in genomic DNA from *wim* embryos and is not present in expressed sequence tags from other mouse strains. This gene is expressed broadly at E9.5 and E10.5 and at high levels in the node of E7.5 embryos (data not shown).

We identified structural motifs in Polaris and Wim by SMART (http://smart.embl-heidelberg.de) and Pfam (http://www.sanger.ac.uk/Software/Pfam/) analysis.

Phenotypic analysis

In situ hybridization and X-Gal staining on whole-mount embryos and immunofluorescence on frozen sections were done as described[14]. For scanning electron microscopy (SEM), we collected embryos at E8.0, fixed them in 2.5% glutaraldehyde in 0.1 M Sorenson's phosphate for >24 h, and dehydrated them through an ethanol series. Samples were processed and observed according to standard procedures[30].

Received 15 May; accepted 3 September 2003; doi:10.1038/nature02061.

1. Rosenbaum, J. L. & Witman, G. B. Intraflagellar transport. *Nature Rev. Mol. Cell Biol.* **3,** 813–825 (2002).
2. Ma, Y. *et al.* Hedgehog-mediated patterning of the mammalian embryo requires transporter-like function of Dispatched. *Cell* **111,** 63–75 (2002).
3. Caspary, T. *et al.* Mouse *Dispatched homolog1* is required for long-range, but not juxtacrine, Hh signaling. *Curr. Biol.* **12,** 1628–1632 (2002).
4. Murcia, N. S. *et al.* The *Oak Ridge polycystic kidney* (*orpk*) disease gene is required for left–right axis determination. *Development* **127,** 2347–2355 (2000).
5. Collignon, J., Varlet, I. & Robertson, E. J. Relationship between asymmetric nodal expression and the direction of embryonic turning. *Nature* **381,** 155–158 (1996).
6. Schimenti, J. C. *et al.* Interdigitated deletion complexes on mouse chromosome 5 induced by irradiation of embryonic stem cells. *Genome Res.* **10,** 1043–1050 (2000).
7. Motoyama, J. *et al.* Differential requirement for Gli2 and Gli3 in ventral neural cell fate specification. *Dev. Biol.* **259,** 150–161 (2003).
8. Chiang, C. *et al.* Cyclopia and defective axial patterning in mice lacking *Sonic hedgehog* gene function. *Nature* **383,** 407–413 (1996).
9. Litingtung, Y. & Chiang, C. Control of Shh activity and signaling in the neural tube. *Dev. Dyn.* **219,** 143–154 (2000).
10. Takeda, S. *et al.* Left-right asymmetry and kinesin superfamily protein KIF3A: new insights in determination of laterality and mesoderm induction by *kif3A*$^{-/-}$ mice analysis. *J. Cell Biol.* **145,** 825–836 (1999).
11. Marszalek, J. R., Ruiz-Lozano, P., Roberts, E., Chien, K. R. & Goldstein, L. S. *Situs inversus* and embryonic ciliary morphogenesis defects in mouse mutants lacking the KIF3A subunit of kinesin-II. *Proc. Natl Acad. Sci. USA* **96,** 5043–5048 (1999).
12. Goodrich, L. V., Milenkovic, L., Higgins, K. M. & Scott, M. P. Altered neural cell fates and medulloblastoma in mouse *patched* mutants. *Science* **277,** 1109–1113 (1997).
13. Eggenschwiler, J. T., Espinoza, E. & Anderson, K. V. Rab23 is an essential negative regulator of the mouse Sonic hedgehog signalling pathway. *Nature* **412,** 194–198 (2001).
14. Eggenschwiler, J. T. & Anderson, K. V. Dorsal and lateral fates in the mouse neural tube require the cell-autonomous activity of the *open brain* gene. *Dev. Biol.* **227,** 648–660 (2000).
15. Wang, B., Fallon, J. F. & Beachy, P. A. Hedgehog-regulated processing of Gli3 produces an anterior/posterior repressor gradient in the developing vertebrate limb. *Cell* **100,** 423–434 (2000).
16. Litingtung, Y. & Chiang, C. Specification of ventral neuron types is mediated by an antagonistic interaction between Shh and Gli3. *Nature Neurosci.* **3,** 979–985 (2000).
17. Wheatley, D. N., Wang, A. M. & Strugnell, G. E. Expression of primary cilia in mammalian cells. *Cell Biol. Int.* **20,** 73–81 (1996).
18. Sisson, J. C., Ho, K. S., Suyama, K. & Scott, M. P. Costal2, a novel kinesin-related protein in the Hedgehog signaling pathway. *Cell* **90,** 235–245 (1997).
19. Ray, K. *et al.* Kinesin-II is required for axonal transport of choline acetyltransferase in *Drosophila*. *J. Cell Biol.* **147,** 507–518 (1999).
20. Han, Y., Kwok, B. H. & Kernan, M. J. Intraflagellar transport is required in *Drosophila* to differentiate sensory cilia but not sperm. *Curr. Biol.* **13,** 1679–1686 (2003).
21. Bale, A. E. Hedgehog signaling and human disease. *Annu. Rev. Genom. Hum. Genet.* **3,** 47–65 (2002).
22. Sloboda, R. D. A healthy understanding of intraflagellar transport. *Cell Motil. Cytoskeleton* **52,** 1–8 (2002).
23. Kasarskis, A., Manova, K. & Anderson, K. V. A phenotype-based screen for embryonic lethal mutations in the mouse. *Proc. Natl Acad. Sci. USA* **95,** 7485–7490 (1998).
24. Hui, C. C. & Joyner, A. L. A mouse model of Greig cephalopolysyndactyly syndrome: the *extra-toes*^{J} mutation contains an intragenic deletion of the *Gli3* gene. *Nature Genet.* **3,** 241–246 (1993).
25. Cole, T. B., Wenzel, H. J., Kafer, K. E., Schwartzkroin, P. A. & Palmiter, R. D. Elimination of zinc from synaptic vesicles in the intact mouse brain by disruption of the *ZnT3* gene. *Proc. Natl Acad. Sci. USA* **96,** 1716–1721 (1999).
26. Vetter, D. E. *et al.* Urocortin-deficient mice show hearing impairment and increased anxiety-like behavior. *Nature Genet.* **31,** 363–369 (2002).
27. Weiher, H., Noda, T., Gray, D. A., Sharpe, A. H. & Jaenisch, R. Transgenic mouse model of kidney disease: insertional inactivation of ubiquitously expressed gene leads to nephrotic syndrome. *Cell* **62,** 425–434 (1990).
28. Farrelly, D. *et al.* Mice mutant for glucokinase regulatory protein exhibit decreased liver glucokinase: a sequestration mechanism in metabolic regulation. *Proc. Natl Acad. Sci. USA* **96,** 14511–14516 (1999).
29. Howard, P. W. & Maurer, R. A. Identification of a conserved protein that interacts with specific LIM homeodomain transcription factors. *J. Biol. Chem.* **275,** 13336–13342 (2000).
30. Sulik, K. *et al.* Morphogenesis of the murine node and notochordal plate. *Dev. Dyn.* **201,** 260–278 (1994).

Supplementary Information accompanies the paper on **www.nature.com/nature**.

Acknowledgements We thank K. Maxwell and T. Caspary for initial experiments with *fxo*; N. Lampen for assistance with SEM; J. Eggenschwiler, D. Cole and M. Kernan for sharing unpublished data; C. Sander and B. Reva for discussions about Wim and Polaris protein structures; T. Bestor, T. Caspary, J. Eggenschwiler, M. García-García and J. Lee for comments on the manuscript; E. Robertson, M. Scott and J. Schimenti for mice; and C. Cepko for the Chx10 antibody. Monoclonal antibodies were obtained from the Developmental Studies Hybridoma Bank, which was developed under the auspices of the National Institute of Child Health and Human Development and is maintained by The University of Iowa, Department of Biological Sciences. Genome sequence analysis used Ensembl and the Celera Discovery System and associated databases, made possible in part by the AMDeC Foundation. This work was supported by NIH grants to K.V.A. and the Lita Annenberg Hazen Foundation. L.N. is an Investigator of the Howard Hughes Medical Institute.

Competing interests statement The authors declare that they have no competing financial interests.

Correspondence and requests for materials should be addressed to K.V.A. (k-anderson@ski.mskcc.org). The *wim* complementary DNA sequence is deposited in GenBank under accession number AY339616.

Degradation of Cdc25A by β-TrCP during S phase and in response to DNA damage

Luca Busino[1]*, Maddalena Donzelli[1]*, Massimo Chiesa[1], Daniele Guardavaccaro[2], Dvora Ganoth[3], N. Valerio Dorrello[2], Avram Hershko[3], Michele Pagano[2] & Giulio F. Draetta[1]

[1]*European Institute of Oncology, 435 Via Ripamonti, 20141 Milan, Italy*
[2]*Department of Pathology, MSB 599, New York University School of Medicine and NYU Cancer Institute, 550 First Avenue, New York, New York 10016, USA*
[3]*Unit of Biochemistry, B. Rappaport Faculty of Medicine, Technion-Israel Institute of Technology, Haifa 31096, Israel*

* These authors equally contributed to this work

The Cdc25A phosphatase is essential for cell-cycle progression because of its function in dephosphorylating cyclin-dependent kinases. In response to DNA damage or stalled replication, the ATM and ATR protein kinases activate the checkpoint kinases Chk1 and Chk2, which leads to hyperphosphorylation of Cdc25A[1–3]. These events stimulate the ubiquitin-mediated proteolysis of Cdc25A[1,4,5] and contribute to delaying cell-cycle progression, thereby preventing genomic instability[1–7]. Here we report that β-TrCP is the F-box protein that targets phosphorylated Cdc25A for degradation by the Skp1/Cul1/F-box protein complex. Downregulation of β-TrCP1 and β-TrCP2 expression by short interfering RNAs causes an accumulation of Cdc25A in cells progressing through S phase and prevents the degradation of Cdc25A induced by ionizing radiation, indicating that β-TrCP may function in the intra-S-phase checkpoint. Consistent with

this hypothesis, suppression of β-TrCP expression results in radioresistant DNA synthesis in response to DNA damage—a phenotype indicative of a defect in the intra-S-phase checkpoint that is associated with an inability to regulate Cdc25A properly. Our results show that β-TrCP has a crucial role in mediating the response to DNA damage through Cdc25A degradation.

We previously showed that the ubiquitin-mediated degradation of Cdc25A at the exit of mitosis is mediated by the anaphase promoting complex/cyclosome (APC/C^{Cdh1}) ubiquitin ligase through recognition of a specific KEN box sequence[8]. We also showed that a Cdc25A KEN mutant is resistant to APC-mediated ubiquitination but remains short-lived in interphase cells like the wild-type protein and is still degraded in response to ionizing radiation, thereby suggesting that Cdc25A may be targeted for degradation by a dual mechanism[8]. Furthermore, degradation of Cdc25A both in cycling cells and in response to DNA damage depends on phosphorylation[1–4], which is also a requirement for the efficient recruitment of target proteins to Skp1/Cullin/F-box (SCF) ubiquitin ligases by F-box proteins[9,10], as reported for other cell-cycle regulators (reviewed in ref. 11).

We previously established that Cdc25A is in complex with Cul1 and Skp1 (ref. 8), which prompted us to examine the possible involvement of SCF in the degradation of Cdc25A. To achieve this, we screened several human F-box proteins[12,13] for interaction with Cdc25A. We observed that β-TrCP1 and β-TrCP2 (also known as Fbw1a and Fbw1b, respectively) were the only F-box proteins among those tested, namely Fbw2, Fbw4, Fbw5 and Fbw7, that interacted with Cdc25A *in vivo* (Fig. 1a and data not shown for Skp2 and Fbl3). As a control, we assessed that the Cul1 subunit was bound to all of the F-box proteins tested. In a parallel experiment, we showed that overexpressed Cdc25A coprecipitates with β-TrCP1 and β-TrCP2 (hereafter β-TrCP1/2), but not with Skp2 and Fbw7 (Fig. 1b). Notably, the Cdc25A that co-precipitated with β-TrCP1/2 was hyperphosphorylated, because treatment of the immunocomplexes with λ-phosphatase generated a faster migrating band of Cdc25A (Fig. 1c).

The Cdc25A amino acid sequence contains a motif, DSGXXXXS (DSG$(X)_4$S), which is similar to the DSGXXS or DSGXXXS motifs present in known protein substrates of the $SCF^{β\text{-}TrCP}$ complex (refs 14–17 and Fig. 2a). Phosphorylation at both serine residues is required both for β-TrCP binding and for subsequent substrate degradation[15,18]. To assess the contribution of this motif to the interaction, we mutated Ser 82 and Ser 88 to alanine, either alone to generate a $Cdc25A^{DSG2×}$ mutant, or in addition to the preceding Ser 79 to produce a $Cdc25A^{DSG3×}$ mutant (Fig. 2a). We then tested whether these mutated proteins would interact with β-TrCP in transfected cells.

Replacement of the two DSG$(X)_4$S serines with alanine was sufficient to abolish Cdc25A interaction with β-TrCP1 (Fig. 2b). This interaction is probably dependent on phosphorylation on the DSG$(X)_4$S serine residues. Indeed, a Cdc25A-derived peptide containing phosphoserine residues at positions Ser 82 and Ser 88 (Fig. 2a) associated with *in vitro* translated β-TrCP1/2, but not with other F-box proteins tested, whereas the unphosphorylated peptide did not associate at all (Fig. 2c). We also assessed whether a failure to interact with β-TrCP would affect the stability of Cdc25A. We determined the half-life of $Cdc25A^{DSG2×}$ and $Cdc25A^{DSG3×}$ and found that the mutants were considerably more stable than wild-type Cdc25A (Fig. 2d).

To investigate whether β-TrCP stimulates ubiquitination of Cdc25A, we carried out an *in vitro* ubiquitination assay using partially reconstituted HeLa cell extracts. Addition of recombinant purified β-TrCP1, but not two other F-box proteins (Skp2 and Fbw7), stimulated ubiquitination of Cdc25A (Fig. 2e). Ubiquitination by β-TrCP also required protein phosphorylation, because the reaction was inhibited by replacing ATP with AMP-PNP, an analogue that allows ubiquitin adenylation by E1 ligase but cannot function as a protein kinase substrate (Fig. 2f). As a control, AMP-PNP facilitated APC-dependent ubiquitination, which does not require substrate phosphorylation (data not shown). These data support the hypothesis that Cdc25A phosphorylation is required for β-TrCP-mediated ubiquitination. Notably, β-TrCP1-mediated ubiquitination of $Cdc25A^{DSG3×}$ was greatly affected as compared with wild-type Cdc25A (Fig. 2g). Together, these data indicate that phosphorylation on Ser 82 and Ser 88 is required for efficient recruitment of Cdc25A by β-TrCP and its subsequent degradation.

We used a series of siRNA experiments to assess further the role of β-TrCP in controlling the subcellular abundance of Cdc25A. Asynchronously growing cells were transiently transfected with an siRNA oligonucleotide targeting both β-TrCP1 and β-TrCP2 genes and analysed for steady-state amounts of Cdc25A. Efficient silencing of β-TrCP1/2 caused a considerable accumulation of Cdc25A as compared with mock-transfected cells (Fig. 3a). No substantial changes were observed in Cdc25A messenger RNA (Fig. 3a).

We then tested the effect of silencing β-TrCP gene expression at various stages of the cell cycle. Cells that were mock-transfected or transfected with β-TrCP1/2 siRNA were synchronized by double-

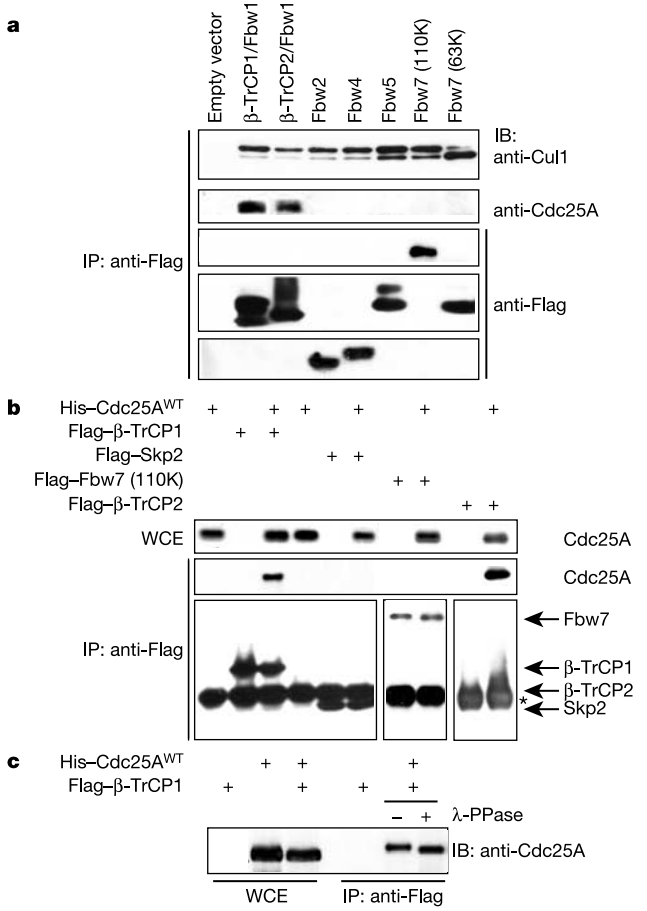

Figure 1 Cdc25A interacts with β-TrCP1 and β-TrCP2 *in vivo*. **a**, HeLa cells were transfected with the indicated Flag–tagged F-box protein constructs. F-box proteins were immunoprecipitated from extracts with an anti-Flag resin and immunocomplexes were blotted with antibodies specific for Cul1, Cdc25A and Flag. **b**, HeLa cells were co-transfected with a vector expressing His–Cdc25A plus the indicated Flag-tagged F-box protein constructs. Immunocomplexes were analysed as in **a**. WCE, whole-cell extract. Asterisk indicates the position of the IgG heavy chain (β-TrCP2 protein overlaps with IgG). **c**, Cdc25A bound to β-TrCP proteins is phosphorylated. Immunocomplexes obtained by β-TrCP1 immunoprecipitation were treated with λ-phosphatase and analysed for Cdc25A.

thymidine treatment, released from G1/S arrest in the presence of nocodazole and analysed over time for Cdc25A. As they progressed through S phase, cells treated with β-TrCP1/2 siRNA showed a substantial accumulation of Cdc25A as compared to mock-transfected cells, as well as a failure to degrade the APC inhibitor Emi1 (also known as Fbx5), a target of β-TrCP in early mitosis (refs 19, 20 and Fig. 3b).

To analyse the kinetics of Cdc25A expression at mitotic exit and in G1 phase, mock-transfected or cells transfected with β-TrCP1/2 siRNA were synchronized by nocodazole treatment, released from the mitotic block and analysed over time for Cdc25A. Cells transfected with β-TrCP1/2 siRNA had substantially more Cdc25A at mitosis than did mock-transfected cells, but similar to control cells they proceeded normally into G1 phase and degraded both Cdc25A and cyclin B1, albeit with slower kinetics (Fig. 3c). This behaviour is probably caused by an increase in Emi1 in cells transfected with β-TrCP siRNA[19,20], resulting in an indirect up-regulation of Cdc25A through inhibition of Cdh1 at the exit of mitosis[21].

We directly compared the amounts of Cdc25A in mock-transfected and cells transfected with β-TrCP1/2 and Emi1 siRNA at different time points (Fig. 3b, c, right). Elimination of β-TrCP caused an accumulation of Cdc25A in all cell-cycle phases apart from G1 (Fig. 3c, T6). As a control, we verified that elimination of

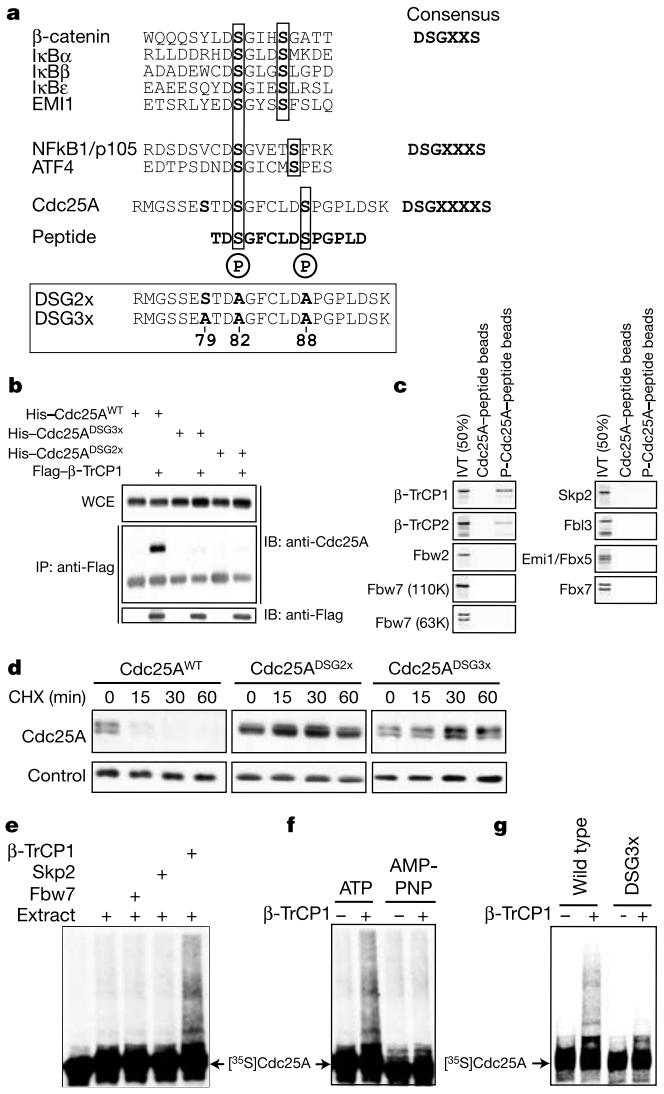

Figure 2 Interaction with β-TrCP protein through a phosphorylated DSG motif is required for Cdc25A degradation and polyubiquitination. **a**, Alignment of DSG motifs identified in known β-TrCP substrates. Serine-to-alanine mutations in the DSG motif of Cdc25A are boxed. **b**, Vectors expressing His-tagged Cdc25A$^{DSG2\times}$ and Cdc25A$^{DSG3\times}$ were coexpressed with Flag–β-TrCP1 in HeLa cells, and anti-Flag immunocomplexes were blotted for Cdc25A. **c**, Immobilized Cdc25A-derived peptides, with or without phosphorylation on Ser 82 and Ser 88 (**a**), were incubated with [^{35}S]methionine-labelled *in vitro* translated F-box proteins (IVT) and analysed by autoradiography. **d**, HeLa cells were transfected with the indicated Flag-tagged constructs and analysed for Cdc25A expression after cycloheximide (CHX) treatment. **e**, [^{35}S]methionine-labelled *in vitro* translated Cdc25A was incubated with HeLa cell extract enriched with the indicated Skp1–F-box protein complexes and analysed by autoradiography. **f**, The ATP analogue AMP-PNP was used in the ubiquitin ligation reaction. **g**, β-TrCP-mediated ubiquitination of wild-type Cdc25A and the Cdc25A$^{DSG3\times}$ mutant.

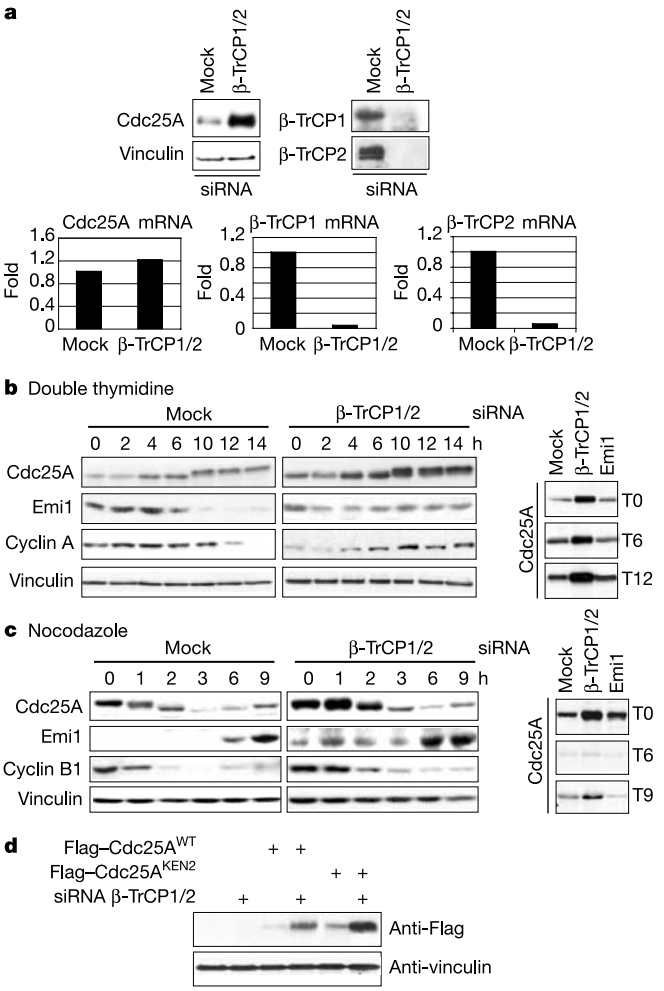

Figure 3 β-TrCP controls Cdc25A abundance during progression of S phase. **a**, HeLa cells were mock-transfected or transfected with β-TrCP1 and β-TrCP2 siRNA oligonucleotides. Expression of Cdc25A and β-TrCP1/2 (analysed by immunoblotting and quantitative PCR) is shown. **b**, Cells transfected as indicated were synchronized by double-thymidine block and released in nocodazole-containing medium. Cells were collected at the indicated time points, lysed and immunoblotted for Cdc25A, Emi1 and cyclin A. Samples collected at the T0, T6 an T12 time points were aligned for a direct comparison of Cdc25A expression. **c**, Cells transfected as indicated were synchronized by nocodazole treatment and released in drug-free medium. Cells were analysed for Cdc25A, Emi1 and cyclin B1 as in **b**. **d**, Cells transfected with a vector expressing Flag-tagged wild-type Cdc25A or a Cdc25A^{KEN2} mutant were subjected to RNA interference and analysed for overexpression of Cdc25A.

Emi1 did not affect the expression of Cdc25A protein. We also observed that the Cdc25A^{KEN2} mutant, which is not degraded by APC/C^{Cdh1}, also accumulated in cells transfected with β-TrCP1/2 siRNA (Fig. 3d). Together, these data indicate that β-TrCP-mediated degradation of Cdc25A may occur throughout S and G2, and that this event is independent of the release of the Emi1-mediated inhibition of Cdh1.

To examine whether β-TrCP proteins are involved in the ubiquitin-mediated degradation of Cdc25A in response to DNA damage, cells transfected with β-TrCP1/2 siRNA were treated with ionizing radiation and analysed for Cdc25A abundance. Cells with reduced β-TrCP1/2 showed an increase in Cdc25A as compared with mock-transfected and Cdh1-depleted cells, which were used as a negative control. Notably, ionizing radiation resulted in an accumulation of slow-migrating, hyperphosphorylated Cdc25A species (Fig. 4a, b). Furthermore, the half-life of Cdc25A in S-phase-synchronized and β-TrCP1/2-depleted cells was extended and remained unmodified in cells treated with ionizing radiation as compared with untreated cells (Fig. 4b).

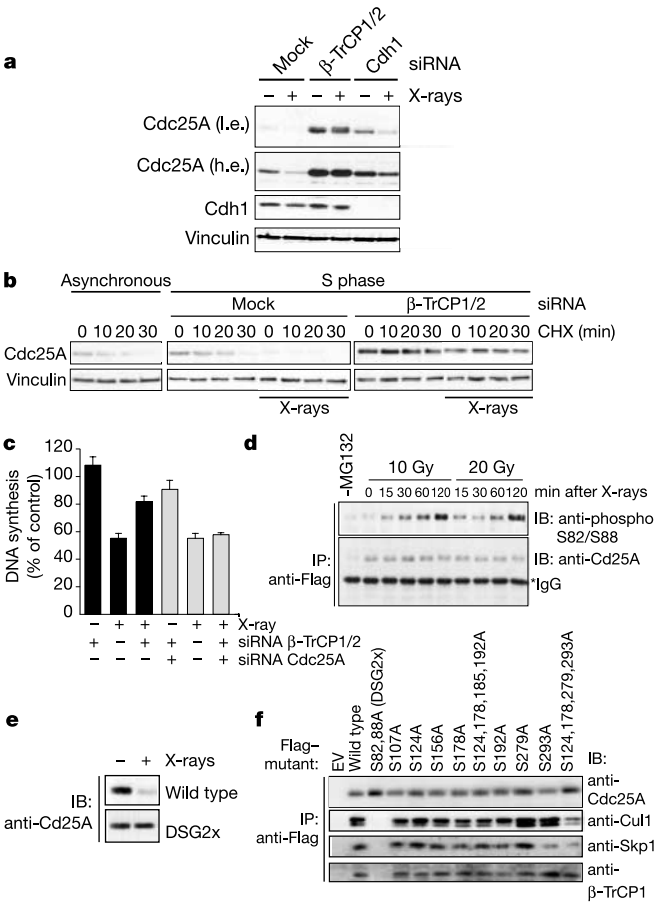

Figure 4 β-TrCP is required for degradation of Cdc25A induced by ionizing radiation in the intra-S-phase checkpoint. **a**, HeLa cells were mock-transfected or transfected with β-TrCP or Cdh1 siRNA and after 48 h were exposed to ionizing radiation (10 Gy). Cdc25A protein is shown at low and high exposure. **b**, siRNA-transfected S-phase cells were exposed to ionizing radiation, and the half-life of Cdc25A was analysed by cycloheximide (CHX) treatment. **c**, Percentage of DNA synthesis, normalized against mock-transfected non-irradiated cells, was assessed in mock-transfected cells and in cells transfected with β-TrCP1/2 or β-TrCP1/2 plus Cdc25A siRNA, 90 min after ionizing radiation treatment. **d**, HeLa cells overexpressing Flag–Cdc25A were irradiated with 10 and 20 Gy in the presence of the proteasome inhibitor MG132 and collected at the indicated time points after irradiation. Immunoprecipitated Cdc25A was immunoblotted with a purified anti-phosphoS82/S88 antibody. **e**, U2OS cells stably expressing wild-type Cdc25A or Cdc25A$^{DSG2\times}$ were mock-treated or treated by ionizing radiation. **f**, Flag-tagged Cdc25A immunocomplexes were immunoblotted for Cdc25A, Cul1, Skp1 and β-TrCP1.

To establish a role for β-TrCP in the Cdc25A-mediated DNA damage response, we examined whether interfering with β-TrCP expression would result in a defect in the temporal inhibition of DNA synthesis. Radioresistant DNA synthesis (RDS), a phenotype indicative of a defective intra-S-phase checkpoint, occurs in cells deficient for ATM and Chk2, two upstream negative effectors of Cdc25A abundance[1,22]. We checked for the integrity of the intra-S-phase checkpoint in cells transfected with β-TrCP siRNA by assessing their rate of DNA synthesis after treatment with ionizing radiation. Whereas mock-transfected cells showed an inhibition of DNA synthesis of about 40–50% after ionizing radiation, β-TrCP1/2-depleted cells showed an inhibition of roughly 20%, consistent with an RDS phenotype (Fig. 4c). This effect was dependent on an accumulation of Cdc25A caused by β-TrCP inhibition, given that cells depleted for both β-TrCP and Cdc25A rescued the RDS phenotype.

Using a polyclonal antibody raised against the phosphorylated DSG motif of Cdc25A (anti-phosphoS82/S88) and phosphopeptide mapping, we detected Cdc25A phosphorylation at the DSG motif in cycling cells (Supplementary Figs 1 and 2). DSG phosphorylation was stimulated on treatment with ionizing radiation (Fig 4d). It therefore seems that Cdc25A is phosphorylated at the DSG motif in cycling cells and that this process is enhanced on DNA damage. Indeed, expression of the Cdc25A$^{DSG2\times}$ mutant hampered Cdc25A degradation on treatment with ionizing radiation (Fig 4e).

Cdc25A is phosphorylated on specific serine residues by the Chk1 protein kinase in cycling cells and by both Chk1 and Chk2 in checkpoint activated cells[3], and disruption of the Chk1/Cdc25A pathway abrogates S and G2 checkpoints induced by ionizing radiation[2,3]. Combined mutation of these residues confers stability to the protein, suggesting that phosphorylation at several sites contributes to Cdc25A degradation *in vivo*[3]. These findings might indicate that, as in the recognition of Sic1 by Fbw7 (ref. 23), multiple phosphorylation events on the target protein enhance its interaction with the F-box protein and stimulate its polyubiquitination[24]. For Cdc25A, we found that whereas the Cdc25A$^{DSG2\times}$ mutant failed to form complexes *in vivo* with β-TrCP1, Skp1 or Cul1, none of the Chk1/2 phosphorylation site mutants was impaired in binding these SCF components (Fig. 4f). The finding that the DSG motif is required for β-TrCP binding (Fig. 4f) and for β-TrCP-dependent ubiquitination (Fig. 2g) implies that efficient Cdc25A recognition by β-TrCP minimally requires two phosphorylation sites in Cdc25A. This is in agreement with the three-dimensional structure of a β-TrCP1–Skp1–β-catenin complex[25]. Phosphorylation on serine residues other than those in the DSG motif[5] might stimulate the degradation of Cdc25A by facilitating an interaction with additional components of the SCF complex, or by enhancing the ability of SCF to catalyse polyubiquitination.

We have shown a requirement for β-TrCP proteins in regulating Cdc25A ubiquitination in S phase and on treatment with ionizing radiation. Notably, a gain-of-function mutation in the *cdc25* gene of *Caenorhabditis elegans* results in deregulated hyperproliferation of intestinal cells[26]. The encoded mutated protein carries a serine-to-phenylalanine substitution in a putative DSG consensus. Given the fact that mutations in ATM and ATR, which are upstream negative effectors of Cdc25A, are common in cancer[22,27], an assessment of the occurrence of activating mutations in the Cdc25A gene and/or inactivating mutations in the β-TrCP genes in normal and tumour tissues should be warranted. □

Methods

Cell culture, synchronization and transfection

Cell culture, cell synchronization and transfection protocols were done as described[8].

Plasmids

Flag- and His-tagged Cdc25A mutants were generated using the QuickChange Site-directed Mutagenesis kit (Stratagene). We verified all constructs by DNA sequencing.

Immunoblotting, immunoprecipitation and phosphatase treatment

Immunoblotting and immunoprecipitation were done essentially as described[8], with the following antibodies: anti-Cdc25A (F6, Santa Cruz Biotech); anti-Flag (M2, Sigma); anti-Cul1 (Zymed); anti-cyclinB1 (GNS1, Santa Cruz Biotech); anti-cyclinA (H-432, Santa Cruz Biotech); anti-Myc (9E10, Santa Cruz Biotech); anti-vinculin (Sigma); anti-Skp1 (1C10F4, Zymed); anti-β-TrCP1 (M.P.'s polyclonal serum); anti-β-TrCP2 (N-15, Santa Cruz Biotech); Anti-Emi1 antibodies were provided by P. K. Jackson (Stanford Univ. School of Medicine), and anti-Cdh1 monoclonal antibodies were supplied by K. Helin (European Inst. Oncology).

For phosphatase treatment, 500 units of λ protein phosphatase (New England Biolabs) was added to β-TrCP immunocomplexes in the presence of $MgCl_2$ for 30 min at 30 °C.

Peptide-binding assay

We obtained two peptides corresponding to the amino acid sequence TDSGFCLDSPGPLD of human Cdc25A (Eurogentec), one of which double-phosphorylated on serine residues. The peptides were coupled to agarose beads using the Aminolink kit (Pierce). Coupled Cdc25A peptides (10 μg) were incubated with [^{35}S]methionine-labelled *in vitro* translated β-TrCP1/2 obtained by the TNT-coupled Reticulocyte Lysate system (Promega) in the presence of 5 μCi of [^{35}S]methionine (Amersham Biosciences). We washed agarose beads with RIPA buffer and assayed binding by SDS–PAGE followed by autoradiography.

In vitro ubiquitination assay

Ubiquitin ligation was determined essentially as described[28] by using [^{35}S]methionine-labelled *in vitro* translated Cdc25A. Baculovirus β-TrCP1, Skp2 or Fbw7 were all coexpressed with His_6–Skp1, purified by nickel-agarose chromatography and added in roughly similar amounts to the reaction.

siRNA

We purchased Cdh1 (ref. 8), β-TrCP1/2 (refs 19, 20), Emi1 (ref. 21) and Cdc25A (ref. 2) 21-base-pair siRNA oligonucleotides (Dharmacon Research). Cells were transfected with siRNA duplexes by using Oligofectamine (Invitrogen) according to the manufacturer's instructions.

Radio-resistant DNA synthesis assay

Cells were transfected with siRNA duplexes, and after 4 h were labelled for 24 h with 20 nCi ml^{-1} [^{14}C]thymidine (Amersham Biosciences) and then incubated in non-radioactive medium for another 24 h. Cells were irradiated with 10 Gy, incubated for 90 min at 37 °C, and pulse-labelled with 5 μCi ml^{-1} [^{3}H]thymidine (Amersham Biosciences) for the last 20 min. The medium was removed and the cells were washed twice with PBS, once with 5% trichloracetic acid and twice with 100% ethanol, and then lysed with 200 μl of buffer containing 1% SDS and 10 mM NaOH. We assayed 150-μl aliquots in a liquid scintillation counter. The resulting ratios of ^{3}H counts per min to ^{14}C counts per min represented a measure of the DNA synthesis.

Received 17 June; accepted 17 September 2003; doi:10.1038/nature02082.

1. Falck, J., Mailand, N., Syljuasen, R. G., Bartek, J. & Lukas, J. The ATM–Chk2–Cdc25A checkpoint pathway guards against radioresistant DNA synthesis. *Nature* **410,** 842–847 (2001).
2. Zhao, H., Watkins, J. L. & Piwnica-Worms, H. Disruption of the checkpoint kinase 1/cell division cycle 25A pathway abrogates ionizing radiation-induced S and G2 checkpoints. *Proc. Natl Acad. Sci. USA* **99,** 14795–14800 (2002).
3. Sorensen, C. S. *et al.* Chk1 regulates the S phase checkpoint by coupling the physiological turnover and ionizing radiation-induced accelerated proteolysis of Cdc25A. *Cancer Cell* **3,** 247–258 (2003).
4. Mailand, N. *et al.* Rapid destruction of human Cdc25A in response to DNA damage. *Science* **288,** 1425–1429 (2000).
5. Molinari, M., Mercurio, C., Dominguez, J., Goubin, F. & Draetta, G. F. Human Cdc25 A inactivation in response to S phase inhibition and its role in preventing premature mitosis. *EMBO Rep.* **1,** 71–79 (2000).
6. Bartek, J. & Lukas, J. Mammalian G1- and S-phase checkpoints in response to DNA damage. *Curr. Opin. Cell Biol.* **13,** 738–747 (2001).
7. Falck, J., Petrini, J. H., Williams, B. R., Lukas, J. & Bartek, J. The DNA damage-dependent intra-S phase checkpoint is regulated by parallel pathways. *Nature Genet.* **30,** 290–294 (2002).
8. Donzelli, M. *et al.* Dual mode of degradation of Cdc25A phosphatase. *EMBO J.* **21,** 4875–4884 (2002).
9. Jackson, P. K. & Eldridge, A. G. The SCF ubiquitin ligase: an extended look. *Mol. Cell* **9,** 923–925 (2002).
10. Patton, E. E., Willems, A. R. & Tyers, M. Combinatorial control in ubiquitin-dependent proteolysis: don't Skp the F-box hypothesis. *Trends Genet.* **14,** 236–243 (1998).
11. Spruck, C. H. & Strohmaier, H. M. Seek and destroy: SCF ubiquitin ligases in mammalian cell cycle control. *Cell Cycle* **1,** 250–254 (2002).
12. Cenciarelli, C. *et al.* Identification of a family of human F-box proteins. *Curr. Biol.* **9,** 1177–1179 (1999).
13. Kipreos, E. T. & Pagano, M. The F-box protein family. *Genome Biol.* **1,** Reviews3002.1–3002.7 [online] ⟨http://genomebiology.com/2000/1/5/reviews/3002⟩ (2000).
14. Yaron, A. *et al.* Identification of the receptor component of the IκBα-ubiquitin ligase. *Nature* **396,** 590–594 (1998).
15. Winston, J. T. *et al.* The SCF β-TRCP–ubiquitin ligase complex associates specifically with phosphorylated destruction motifs in IκBα and β-catenin and stimulates IκBα ubiquitination *in vitro*. *Genes Dev.* **13,** 270–283 (1999).
16. Lassot, I. *et al.* ATF4 degradation relies on a phosphorylation-dependent interaction with the SCF$^{\beta TrCP}$ ubiquitin ligase. *Mol. Cell. Biol.* **21,** 2192–2202 (2001).
17. Lang, V. *et al.* βTrCP-mediated proteolysis of NF-κB1 p105 requires phosphorylation of p105 serines 927 and 932. *Mol. Cell. Biol.* **23,** 402–413 (2003).
18. Liu, C. *et al.* Control of β-catenin phosphorylation/degradation by a dual-kinase mechanism. *Cell* **108,** 837–847 (2002).
19. Guardavaccaro, D. *et al.* Control of meiotic and mitotic progression by the F box protein β-Trcp1 *in vivo*. *Dev. Cell* **4,** 799–812 (2003).
20. Margottin-Goguet, F. *et al.* Prophase destruction of Emi1 by the SCF$^{\beta TrCP/Slimb}$ ubiquitin ligase activates the anaphase promoting complex to allow progression beyond prometaphase. *Dev. Cell* **4,** 813–826 (2003).
21. Hsu, J. Y., Reimann, J. D., Sorensen, C. S., Lukas, J. & Jackson, P. K. E2F-dependent accumulation of hEmi1 regulates S phase entry by inhibiting APC^{Cdh1}. *Nature Cell Biol.* **4,** 358–366 (2002).
22. Painter, R. B. & Young, B. R. Radiosensitivity in ataxia-telangiectasia: a new explanation. *Proc. Natl Acad. Sci. USA* **77,** 7315–7317 (1980).
23. Verma, R. *et al.* Phosphorylation of Sic1p by G1 Cdk required for its degradation and entry into S phase. *Science* **278,** 455–460 (1997).
24. Nash, P. *et al.* Multisite phosphorylation of a CDK inhibitor sets a threshold for the onset of DNA replication. *Nature* **414,** 514–521 (2001).
25. Wu, G. *et al.* Structure of a β-TrCP1–Skp1–β-catenin complex: destruction motif binding and lysine specificity of the SCF$^{\beta\text{-}TrCP1}$ ubiquitin ligase. *Mol. Cell* **11,** 1445–1456 (2003).
26. Clucas, C., Cabello, J., Bussing, I., Schnabel, R. & Johnstone, I. L. Oncogenic potential of a *C. elegans cdc25* gene is demonstrated by a gain-of-function allele. *EMBO J.* **21,** 665–674 (2002).
27. Bell, D. W. *et al.* Heterozygous germ line hCHK2 mutations in Li–Fraumeni syndrome. *Science* **286,** 2528–2531 (1999).
28. Carrano, A. C., Eytan, E., Hershko, A. & Pagano, M. SKP2 is required for ubiquitin-mediated degradation of the CDK inhibitor p27. *Nature Cell Biol.* **1,** 193–199 (1999).

Supplementary Information accompanies the paper on **www.nature.com/nature**.

Acknowledgements We thank T. K. Ko for his contribution; Z. G. Pan and S. Reed for reagents; G. Ossolengo for producing and purifying the anti-phosphoS82/S88 antibody; and M. Squatrito and E. De Billy for discussion. This work was supported by an Italian American Cancer Foundation fellowship and a Susan Komen Breast Cancer Foundation fellowship to D.G.; a Irma Hirschl Scholarship and grants from the NIH to M.P.; and grants from the Italian Association for Cancer Research (AIRC), the Italian Foundation for Cancer Research (FIRC) and Telethon to G.F.D.

Competing interests statement The authors declare that they have no competing financial interests.

Correspondence and requests for materials should be addressed to M.D. (mdonzell@ieo.it).

Structural adaptability in the ligand-binding pocket of the ecdysone hormone receptor

Isabelle M. L. Billas, Thomas Iwema, Jean-Marie Garnier, André Mitschler, Natacha Rochel & Dino Moras

Département de Biologie et de Génomique Structurales, IGBMC, CNRS/INSERM/Université Louis Pasteur, Parc d'Innovation BP10142, 67404 Illkirch cedex, France

The ecdysteroid hormones coordinate the major stages of insect development, notably moulting and metamorphosis, by binding to the ecdysone receptor (EcR); a ligand-inducible nuclear transcription factor[1,2]. To bind either ligand or DNA, EcR must form a heterodimer with ultraspiracle (USP), the homologue of retinoid-X receptor[3–5]. Here we report the crystal structures of the ligand-binding domains of the moth *Heliothis virescens* EcR–USP heterodimer in complex with the ecdysteroid ponasterone A and with a non-steroidal, lepidopteran-specific agonist BYI06830 used in agrochemical pest control. The two structures of EcR–USP emphasize the universality of heterodimerization as a general mechanism common to both vertebrates and invertebrates. Comparison of the EcR structures in complex with steroidal and non-steroidal ligands reveals radically different and only partially overlapping ligand-binding pockets that